Modeling complex chemical effects in turbulent nonpremixed combustion

By Nigel S. A. Smith

1. Motivation

Virtually all of the energy derived from the consumption of combustibles occurs in systems which utilize turbulent fluid motion. Since combustion is largely related to the mixing of fluids and mixing processes are orders of magnitude more rapid when enhanced by turbulent motion, efficiency criteria dictate that chemically powered devices necessarily involve fluid turbulence.

Where combustion occurs concurrently with mixing at an interface between two reactive fluid bodies, this mode of combustion is called *nonpremixed* combustion. This is distinct from *premixed* combustion where flame-fronts propagate into a homogeneous mixture of reactants. These two modes are limiting cases in the range of temporal lag between mixing of reactants and the onset of reaction. Nonpremixed combustion occurs where this lag tends to zero, while premixed combustion occurs where this lag tends to infinity. Many combustion processes are hybrids of these two extremes with finite non-zero lag times.

Turbulent nonpremixed combustion is important from a practical standpoint because it occurs in gas fired boilers, furnaces, waste incinerators, diesel engines, gas turbine combustors, and afterburners etc. To a large extent, past development of these practical systems involved an empirical methodology. Presently, efficiency standards and emission regulations are being further tightened (Correa 1993), and empiricism has had to give way to more fundamental research in order to understand and effectively model practical combustion processes (Pope 1991).

A key element in effective modeling of turbulent combustion is making use of a sufficiently detailed chemical kinetic mechanism. The prediction of pollutant emission such as oxides of nitrogen (NO_x) and sulphur (SO_x), unburned hydrocarbons, and particulates demands the use of detailed chemical mechanisms. It is essential that practical models for turbulent nonpremixed combustion are capable of handling large numbers of 'stiff' chemical species equations.

1.1 Reactive Species Closure problem

A common way of idealizing a turbulent flow field is to decompose it into an averaged flow component and a deviational contribution. The nature of the deviational component depends upon the flow and the averaging scheme, but the object of the decomposition is to be able to understand and predict the development of the average component without detailed knowledge of the deviations present in each realization of the flow.

The classical difficulty faced in modeling turbulent nonpremixed combustion is that of closing the averaged equations for chemically reactive species. The instantaneous equation for the evolution of the mass fraction Y_α of a reactive species α is

the following,

$$\frac{\partial}{\partial t}(\rho Y_\alpha) + \frac{\partial}{\partial x_i}(\rho u_i Y_\alpha) = \frac{\partial}{\partial x_j}(\rho D_\alpha \frac{\partial Y_\alpha}{\partial x_j}) + \rho \dot{w}_\alpha \tag{1}$$

where $\dot{w}_\alpha$ is the net chemical production rate of the species α, and D_α is the corresponding molecular diffusivity where a simplified Fickian approximation has been made to model molecular transport. Applying a traditional averaging scheme, such as density weighted (Favre) unconditional ensemble averaging, yields the following,

$$\frac{\partial}{\partial t}(\bar{\rho}\tilde{Y}_\alpha) + \frac{\partial}{\partial x_i}(\bar{\rho}\widetilde{u_i Y}_\alpha) = \frac{\partial}{\partial x_j}(\bar{\rho} D_\alpha \frac{\widetilde{\partial Y_\alpha}}{\partial x_j}) + \bar{\rho}\tilde{\dot{w}}_\alpha. \tag{2}$$

In order to close the averaged species equation a model must be provided for the averaged source term $\tilde{\dot{w}}_\alpha$. First order closures that evaluate the instantaneous chemical rate expressions with averaged species concentrations and temperature,

$$\tilde{\dot{w}}_\alpha(Y_1, Y_2, \ldots, Y_N, T) \approx \dot{w}_\alpha(\tilde{Y}_1, \tilde{Y}_2, \ldots, \tilde{Y}_N, \tilde{T}) \tag{4}$$

are known to be highly inaccurate in combustion cases of practical interest. The chemical reactions encountered in combustion processes are highly nonlinear, and thus small perturbations in the input parameters can cause very large changes in the computed reaction rate.

1.2 Conditional Moment Closure method

The philosophy underpinning the Conditional Moment Closure (CMC) method, as described by Bilger (1991, 1993), is to minimize the level of perturbations from the mean by averaging the reactive species equations *conditionally* upon a conserved scalar mass fraction. In so doing, the resultant statistical moments account for the variations in fluid concentration which result from turbulent mixing alone. At the expense of adding an additional computational dimension to the modeling problem, conditional averaging allows chemical closure to be achieved for most cases of nonpremixed turbulent combustion.

The average of a fluctuating turbulent quantity A, conditional upon the conserved scalar mixture fraction $\xi(x_i, t)$ being equal to a sample value η, is the following (see Klimenko 1990):

$$< A(x_i, t) \mid \xi(x_i, t) = \eta > \equiv \frac{1}{P_\eta} \int \int A(x_i, t)\delta(\xi(x_i, t) - \eta) dx_i dt \tag{5}$$

In the above definition, P_η is the probability density function of the conserved scalar at the location x_i and time t, and δ denotes the Dirac delta function. In all that follows, the full conditional averaging operator $< \ldots \mid \xi(x_i, t) = \eta >$ will be abbreviated to $< \ldots \mid \eta >$ for the sake of brevity.

Klimenko (1990, 1992) and Bilger (1991, 1993) independently showed that the evolution of the conditional mean mass fraction $Q_\alpha \equiv < Y_\alpha \mid \eta >$ of a reactive species α is governed by the following,

$$< \rho \mid \eta > \frac{\partial Q_\alpha}{\partial t} + < \rho u_i \mid \eta > \frac{\partial Q_\alpha}{\partial x_i} = \frac{1}{2} < \rho\chi \mid \eta > \frac{\partial^2 Q_\alpha}{\partial \eta^2} + < \rho \dot{w}_{\ alpha} \mid \eta > + e_q \tag{6}$$

where the molecular diffusivities of all species are assumed to be uniform. The residual term e_q is a conditional correlation between deviational velocity and mass fraction, which is typically assumed to be small. This assumption is not valid in cases where substantial premixing of the reactants occurs, in which case this term can become very important in the reactive species equation (Bilger 1991).

$$e_q \equiv -\frac{\partial}{\partial x_i}(P_\eta < \rho \mid \eta >< u_i' q_\alpha' \mid \eta >)/P_\eta \tag{7}$$

The symbol χ denotes the instantaneous scalar dissipation rate and is defined (below) in terms of the mixture fraction ξ.

$$\chi \equiv 2D_\xi (\frac{\partial \xi}{\partial x_i})^2 \tag{8}$$

In order to close the CMC scalar equation, means of determining $< \chi \mid \eta >$ and $< \dot{w}_\alpha \mid \eta >$ are required.

Klimenko (1992) (see also Klimenko and Bilger 1992) showed that the conditional mean scalar dissipation rate should be determined from the conserved scalar PDF equation to ensure conservation of mass.

$$\frac{\partial}{\partial t}(< \rho \mid \eta > P_\eta) + \frac{\partial}{\partial x_i}(< \rho u_i \mid \eta > P_\eta) = -\frac{1}{2}\frac{\partial^2}{\partial \eta^2}(< \rho\chi \mid \eta > P_\eta) + e_\xi \tag{9}$$

The residual term e_ξ describes molecular diffusion of the PDF in physical space and is negligible at high Reynolds numbers.

Closure of the chemical source term is achieved via a simple first order approximation involving *conditionally* averaged species mass fractions $< \dot{w}_\alpha \mid \eta > \approx \dot{w}_\alpha(Q_1, \ldots, Q_N, < T \mid \eta >)$. This closure approximation is valid in all cases except where the combustion system is close to extinction, since in those cases deviations from the conditional means are large. In such instances doubly conditioned modeling, using conditions upon mixture fraction and a reaction progress variable, is a suitable course of action (Bilger 1991).

The single greatest advantage of the CMC method over other turbulent nonpremixed combustion models is its ability to cope with very detailed chemical descriptions. When contrasted with the Joint Probability Density Function (JPDF) method (see Pope 1985, 1991) the CMC method only adds a new equation to be solved with each new species rather than an additional dimension to the problem. In comparison to laminar flamelet methods, the CMC method does not require there to be a large separation of characteristic scales between mixing and chemical reaction in order to be applicable.

2. Objectives

The objective of this study was to evaluate the CMC method for turbulent nonpremixed combustion, verify or debunk current model assumptions, and where possible suggest model refinements.

Direct numerical simulations (DNS) of nonpremixed combustion in isotropic decaying turbulence were carried out as a first step in this study. By studying nonpremixed combustion in isotropic turbulence with an isotropic flame distribution, all of the computational grid points can be used in calculating spatially degenerate statistics. These statistics allow important modeling problems to be examined without interference from the extraneous, though also important, complications introduced by mean gradients.

Of key interest in this study is the effectiveness of the first order chemical closure employed by the current CMC methodology in a system which embodies the essential elements of combustion chemistry. In this study one- and two-step chemical mechanisms were employed to describe $H_2 - N_2$ fuel burning in air. The one-step mechanism is composed of the non-carbon step from the two-step wet-CO mechanism of Chung and Williams (1990), and allows for global reaction termination due to radical consumption even though no radical species are actually carried (see below).

$$2H_2 + O_2 \rightarrow 2H_2O \qquad (I')$$

The two-step mechanism carries the crucial radical, monatomic hydrogen (H), and contains distinct reactions for radical formation and consumption. The chemical rate constants for reactions I and II (see below) were also taken from the non-carbon steps of Chung and Williams (1990).

$$3H_2 + O_2 \rightleftharpoons 2H_2O + 2H \qquad (I)$$

$$H + H + M \rightarrow H_2 + M \qquad (II)$$

In addition to the abundance of evidence in chemical kinetic literature, recent DNS studies conducted at the CTR have demonstrated the importance of the explicit calculation of chemical radical species in combustion simulations (see Mantel 1994, Vervisch 1992).

Differential diffusion of reactive scalars in nonpremixed combustion is left unmodeled by both the CMC (Smith 1994) and JPDF methods (Yeung and Pope 1993). Although it is of diminished importance in highly turbulent combustion, practical cases have been found where differential diffusion is significant (see Chen *et al.* 1990, Smith *et al.* 1993, Smith 1994, Bilger 1982). The secondary objective of this study was to observe differential diffusion phenomena by comparing simulations that are identical save for the specification of uniform or non-uniform species molecular diffusivities. These observations are to be used to develop model refinements for the prediction of differential diffusion behavior.

2.1 Modeling method

The spatially degenerate CMC and PDF equations corresponding to statistically isotropic conditions with uniform molecular diffusivities are given below,

$$\frac{\partial Q_\alpha}{\partial t} = \frac{1}{2} < \chi \mid \eta > \frac{\partial^2 Q_\alpha}{\partial \eta^2} + < \dot{w}_\alpha \mid \eta > \tag{10}$$

$$\frac{\partial}{\partial t}(< \rho \mid \eta > P_\eta) = -\frac{1}{2}\frac{\partial^2}{\partial \eta^2}(< \rho\chi \mid \eta > P_\eta) \tag{11}$$

where the conditional averages are taken over the entire domain and residual terms have been neglected.

The CMC equation (Eq. 10) was solved with the conditional mean scalar dissipation rate profile being given by the PDF equation in the following manner:

$$< \chi \mid \eta >= \frac{-2}{< \rho \mid \eta > P_\eta} \int \int \frac{\partial}{\partial t}(< \rho \mid \eta' > P_{\eta'}) d\eta' d\eta' \tag{12}$$

In this study it is possible to use PDF information from the simulation to determine the conditional mean scalar dissipation rate, but in practice this information will not typically be available to the modeler. Following the approximations used in practice, the conserved scalar PDFs were assumed to be clipped Gaussian in form. This assumption reduces the number of degrees of freedom in the PDF to two, namely specification of the conserved scalar mean and variance. Beta functions are an arguably superior assumed form (Girimaji 1991), however Gaussians readily lend themselves to accurate integration (Smith 1994).

In cases where differential diffusion is significant, further terms appear in the CMC and PDF equations. Discussion of differential diffusion modeling is deferred to Section 4.

2.2 Simulation conditions

An upgraded version of the code used by Ruetsch (1994) was employed in the direct numerical simulations. The new code includes a flexible multi-step chemical kinetics module for handling arbitrary thermochemistry. The code retains original features such as the high-order compact finite differencing scheme described by Lele (1992) for spatial differencing, and the third order Runge-Kutta timestepping algorithm of Wray. The Navier-Stokes characteristic boundary conditions described by Poinsot and Lele (1992) are also retained, but this feature was not used in this study due to the periodic nature of the simulation domain.

The simulations performed to date have been two dimensional (129x129) in order to extensively test the new code and simulation conditions, before expending a great deal of computation time on three dimensional simulations.

The turbulent field was initialized using an incompressible phase scrambled kinetic energy spectrum for the velocity components and a conserved scalar. The initialized conserved scalar field can be seen Fig. 1 where black regions denote pure

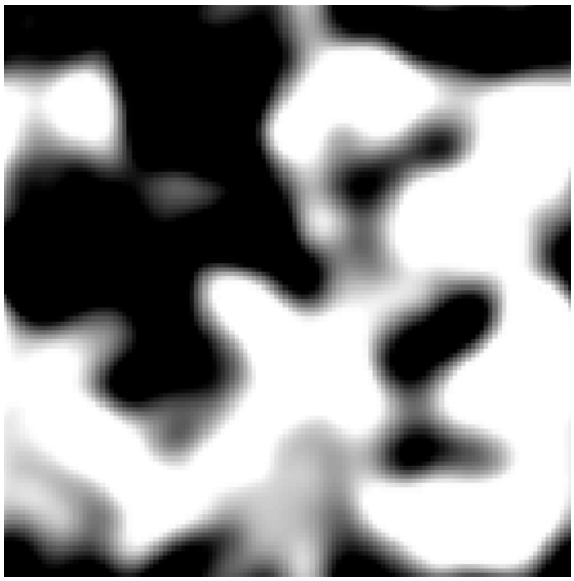

FIGURE 1. Initial distribution of the conserved scalar. White regions denote $\xi = 1$ while black regions denote $\xi = 0$. Initial conserved scalar unmixedness $\Omega = 0.84$.

oxidizer zones and white regions denote pure fuel zones. Scalar *unmixedness* can be defined as,

$$\Omega \equiv < \xi^2 > /(< \xi > (1 - < \xi >)) \tag{14}$$

which can be seen to be a normalized measure of the fluctuation level. Unmixedness varies between zero, where the scalar field is homogeneous, and unity where only pure fuel and pure oxidizer zones exist with no mixing at all. The initial conserved scalar fields used here had initial unmixednesses of $\Omega \approx 0.8$ in all cases.

Reactive species mass fractions and internal energy were mapped onto the conserved scalar field using adiabatic chemical equilibrium relationships between mixture fraction (conserved scalar) and the reactive scalars. The adiabatic equilibrium reactive scalar mass fraction profiles are plotted versus conserved scalar mixture fraction in Fig. 2. Note that the fuel is comprised of almost 97% nitrogen (N_2) by mass, thereby giving a stoichiometric mixture fraction of $\xi_{stoic} = 0.5$. As the mean mixture fraction for the simulations was also 0.5, the overall equivalence ratio was unity in all cases.

The imposition of a 'hot' scalar field onto the initial 'cold' field solution required the adjustment of the density field to minimize the effect on the pressure field. Although the scalar mapping was essentially a constant pressure process, the resultant pressure field had a noticeable acoustic component that arose from the imposed imbalance in the momentum equations. This acoustic adjustment led to an initial root mean square pressure fluctuation that was approximately $5.e-5$ of the mean pressure. Due to periodicity, the acoustic waves were unable to leave the domain but did slowly decrease with time due to dissipation.

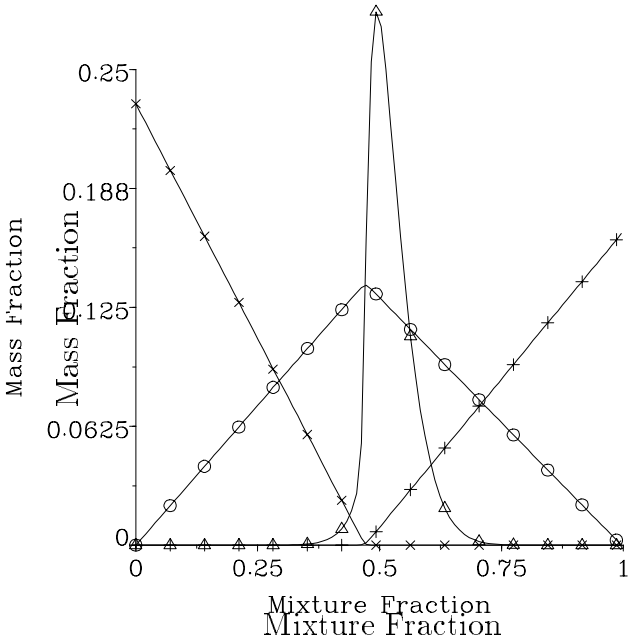

FIGURE 2. Initial conditional mean reactive scalar profiles for two-step chemical description of H_2/N_2-air combustion. Symbol key : $+$ - $H_2(*10)$, $\times$ - O_2, $\circ$ - H_2O, $\triangle$ - $H(*2 \cdot 10^5)$.

3. Results

The general behavior of the numerical simulations can be described as consisting of a brief initial period of chemical and fluid-dynamic adjustment, followed by an extended period of relaxation towards a perfectly mixed quiescent state. The simulations were run over a period of one to two initial turbulent timescales ($\tau_{t,0}$), during which time the conserved scalar unmixedness was found to exponentially decay (see Fig. 3). During the same period the turbulent Reynolds number (determined using the mean viscosity at each time) decreased from ~ 60, to a value of ~ 40.

Due to the chemical reactions taking place between the mixing fluids, the mean temperature and pressure typically rose by a factor of $\sim 4/3$ during the course of each simulation. From Fig. 3, the differences between the one- and two-step chemical calculations can be seen in terms of the mean species yield. It is evident that the one-step chemical description tends to underpredict the overall rate of reaction compared to the two-step case. Despite the fact that both chemical reaction mechanisms cause the system to tend to the same thermodynamic state in the absence of any mixing activity, it is apparent that the global reaction rate predicted by the one-step reduced mechanism is somewhat hindered in the presence of mixing.

In both reaction mechanisms, the chain branching step $H + O_2 \rightleftharpoons OH + O$ is the controlling component in the global rate. The one-step chemical mechanism determines the radical concentration from a quasi-steady state assumption that strictly only holds in the chemical equilibrium limit. Where mixing rates are high, fluid particles do not remain at the same equivalence ratio long enough to allow equilibrium conditions to be reached, and so the quasi-steady state assumption

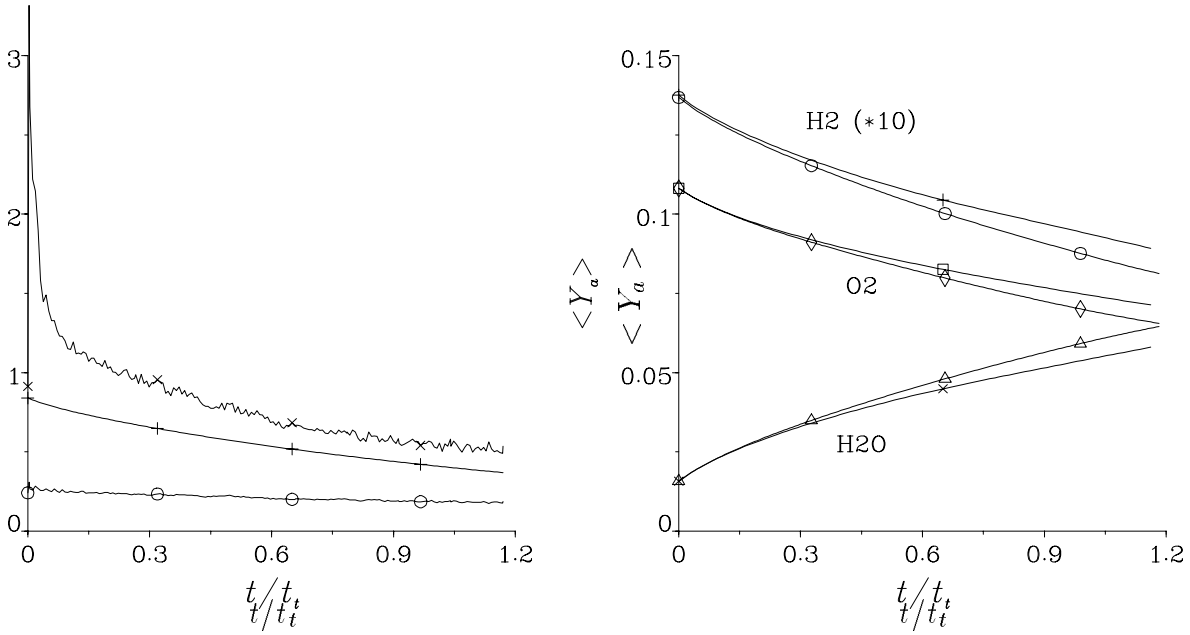

FIGURE 3. Time history of unconditional mean statistics from uniform diffusivity simulations. (Left) Turbulent mixing quantities : + - Ω, $\times$ - $< \epsilon >$ $(*2.5 \cdot 10^{10})$, $\circ$ - $\frac{1}{2} < u_i^2 >$ $(*1 \cdot 10^6)$. (Right) Major species mass fractions for each chemical case : + - one step H_2, $\circ$ - two step H_2, $\sqcap$ - one step O_2, $\diamondsuit$ - two step O_2, $\times$ - one step H_2O, $\triangle$ - two step H_2O

breaks down. The two-step mechanism on the other hand carries H as a computed species, and is not subject to this assumption. It would seem that the one-step prediction of H radical levels is lower than it should be under the mixing rates studied here, and this in turn limits the global reaction rate.

The simulations with non-uniform molecular diffusivities displayed slightly different behavior to that discussed above. Discussion of non-uniform diffusivity effects is deferred to Section 3.2.

3.1 Model results for uniform diffusivity cases

The level of mixing intensity in the CMC model equations is described by the conditional mean scalar dissipation rate. It is important to accurately predict this quantity since it often closely balances the chemical production source terms (see Bilger 1989, Smith 1994). The conditional mean scalar dissipation rate profiles predicted by the model and observed in the companion simulations are plotted in Fig. 4 at three time stations $t/\tau_t = 1/3, 2/3$, and 1. The conditional variance profiles of scalar dissipation rate are also plotted from the simulation data as an indication of the scatter in instantaneous dissipation rate from the conditional means. This scatter is not modeled and is a potential source of inaccuracy.

It is apparent that despite the rather crude assumed-form PDF model used in computing the conditional mean scalar dissipation rate, the agreement with the observed profiles is quite reasonable. The most notable difference being the tendency of the predicted profiles to be greater than the observed profiles at very lean and

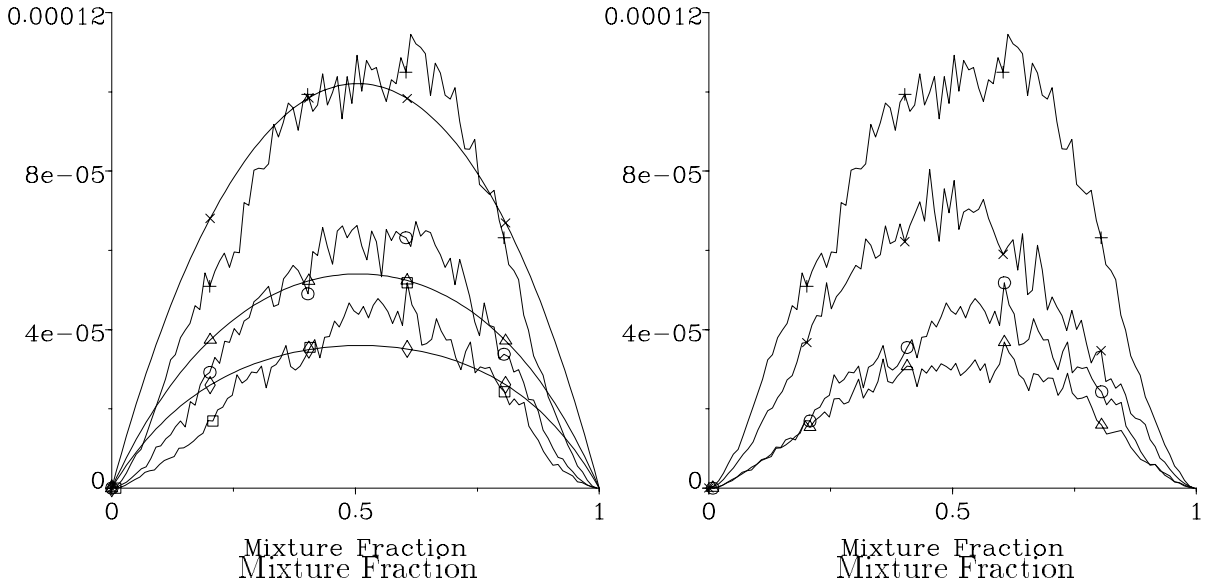

FIGURE 4. (Left) Comparison of modeled and observed conditional mean scalar dissipation rate $< \chi \mid \eta >$ profiles at different calculation times: $+$ - DNS at $t/\tau_t = 1/3$, $\times$ - CMC at $t/\tau_t = 1/3$, $\circ$ - DNS at $t/\tau_t = 2/3$, $\triangle$ - CMC at $t/\tau_t = 2/3$, $\sqcap$ - DNS at $t/\tau_t = 1$, and $\diamondsuit$ - CMC at $t/\tau_t = 1$ (Right) Comparison of observed conditional mean and RMS profiles of scalar dissipation rate at two different calculation times: $+$ - mean at $t/\tau_t = 1/3$, $\times$ - rms at $t/\tau_t = 1/3$, $\circ$ - mean at $t/\tau_t = 1$, and $\triangle$ - rms at $t/\tau_t = 1$.

very rich mixture fractions.

3.1.1 One-step chemical mechanism case

In Fig. 5, conditional mean temperature and H_2O mass fraction profiles are compared between CMC model predictions and simulation data. It is clear that the conditional mean profiles predicted by the model substantially exceed the profiles measured in the DNS. Further, the predicted profiles increase in magnitude with increasing time while the measured conditional mean profiles remain approximately stationary.

The root mean square deviations from the conditional mean profiles, measured in the DNS, increase in magnitude with increasing time. These deviations are not accounted for in the simple first order chemical closure currently used in the CMC model. It seems that these deviations from the conditional mean profiles are sufficient to cause the observed DNS conditional mean reaction rate to be substantially lower than the reaction rate modeled using conditional mean scalar profiles.

Comparing the time histories of the one step chemistry model predictions and simulation results (see Fig. 6), it is apparent that the relative discrepancy between the unconditional mean profiles increases with time. The principal reason for this is that the mixing field slowly tends towards homogeneity, and thus conditional profile discrepancies near the mean mixture fraction become more prominent in the

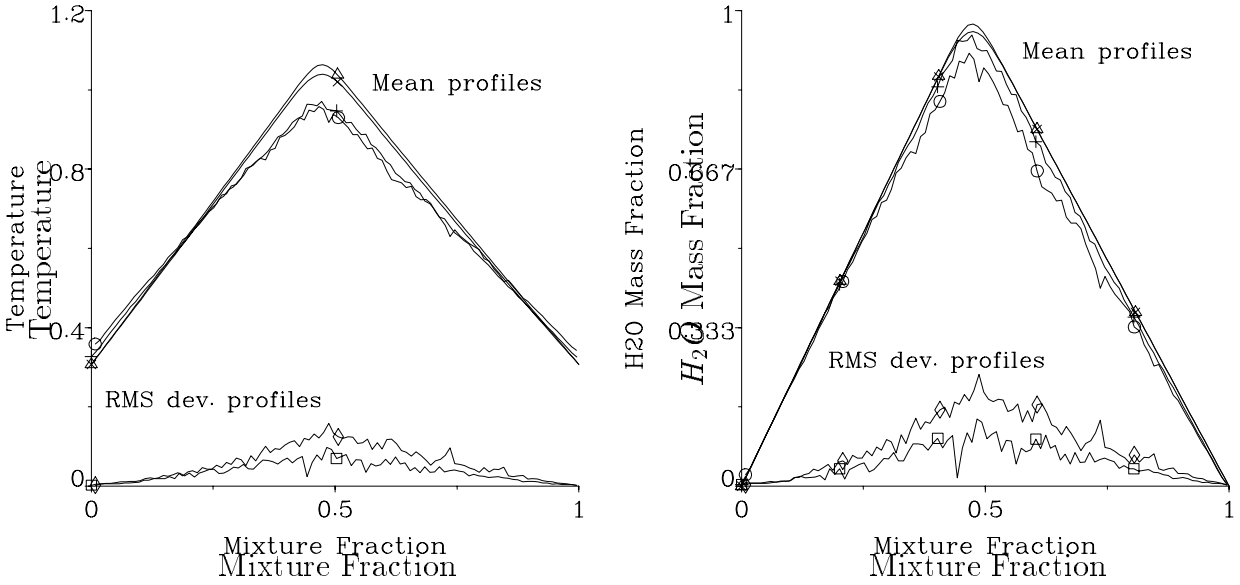

FIGURE 5. Comparison of modeled and observed conditional statistics of temperature (left) and H_2O mass fraction (right) at different calculation times. + - DNS at $t/\tau_t = 1/3$, $\times$ - CMC at $t/\tau_t = 1/3$, $\circ$ - DNS at $t/\tau_t = 1$, $\triangle$ - CMC at $t/\tau_t = 1$, $\sqcap$ - DNS at $t/\tau_t = 1/3$, and $\diamondsuit$ - DNS at $t/\tau_t = 1$

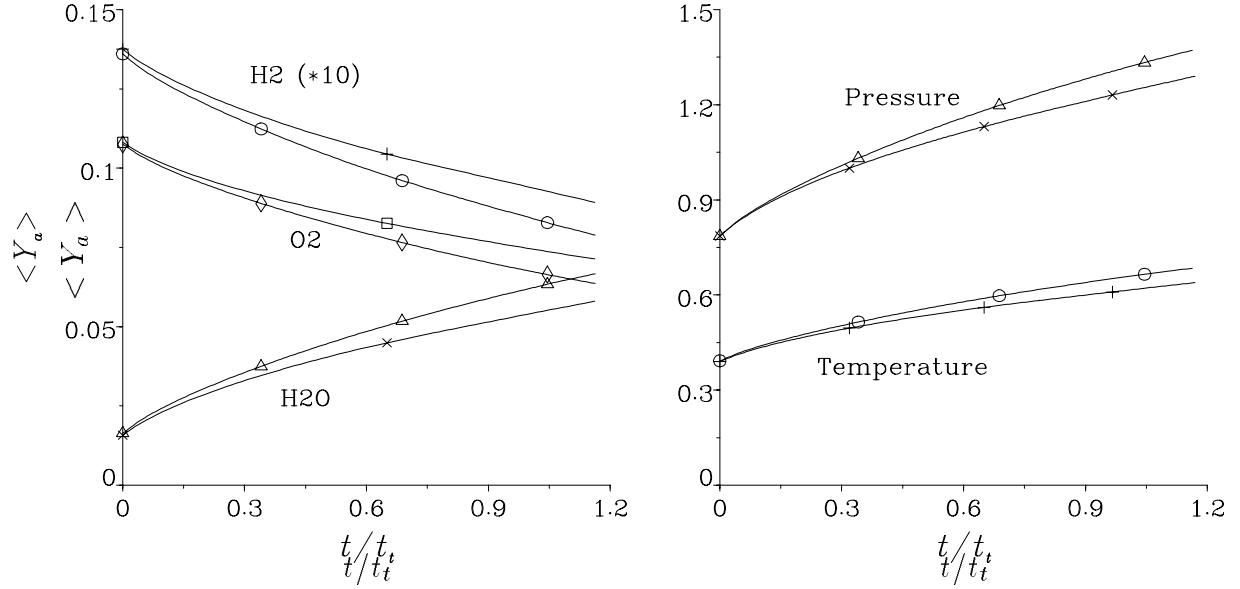

FIGURE 6. Time history of unconditional mean chemical yields from one-step chemistry cases of model and simulation : (Left) + - DNS $H_2(*10)$, $\circ$ - CMC $H_2(*10)$, $\times$ - DNS H_2O, $\triangle$ - CMC H_2O, $\sqcap$ - DNS O_2, $\diamondsuit$ - CMC O_2. (Right) x - DNS pressure, $\triangle$ - CMC pressure, + - DNS temperature, $\circ$ - CMC temperature.

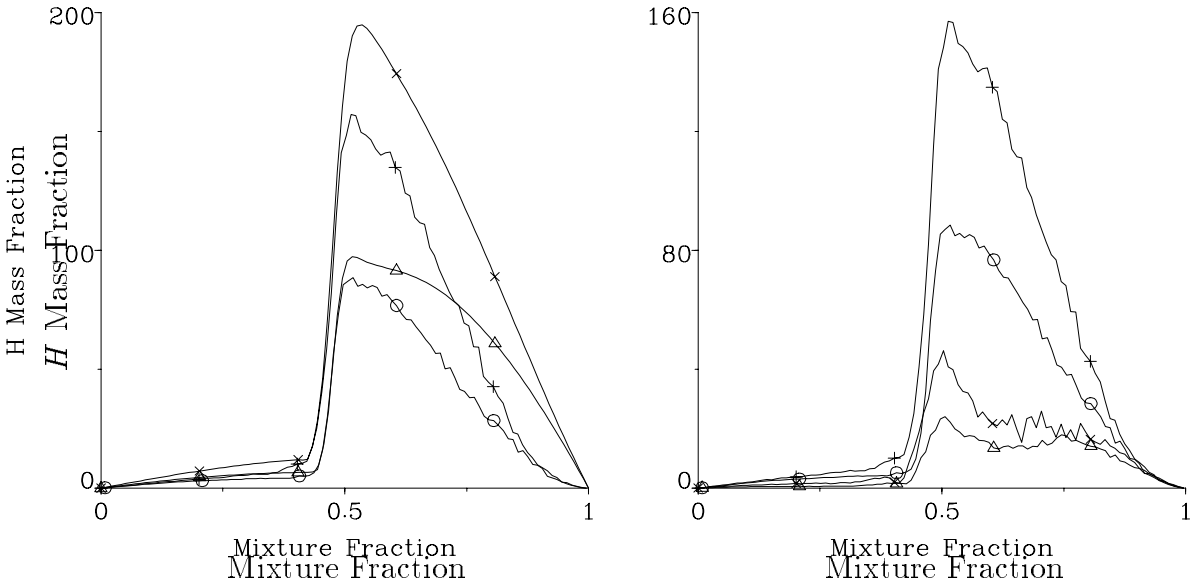

FIGURE 7. Comparison of modeled and observed conditional statistics for H radical mass fraction at different calculation times. (Left) Mean modeled and observed profiles : + - DNS at $t/\tau_t = 1/3$, $\times$ - CMC at $t/\tau_t = 1/3$, $\circ$ - DNS at $t/\tau_t = 1$, $\triangle$ - CMC at $t/\tau_t = 1$. (Right) Mean and RMS deviations from DNS : + - mean at $t/\tau_t = 1/3$, $\times$ - mean at $t/\tau_t = 1$, $\circ$ - RMS dev. at $t/\tau_t = 1/3$, $\triangle$ - RMS dev. at $t/\tau_t = 1$.

convolution with the PDF.

Additionally there is a compounding effect of differences in mean pressure and temperature. The model tends to overpredict the heat release rate as a consequence of the first order chemical closure employed, and this in turn leads to overpredictions of temperature and mean pressure. This departure increases because the elevated temperatures and pressures cause even greater predicted heat release rates. It should be pointed out, however, that the model and simulation trends should converge given a sufficiently long time due to the limited amount of fuel and oxidizer present, and the fact that mixing motions will eventually disappear.

3.1.2 Two-step chemical mechanism case

The discrepancies between model and observation are significantly reduced in the cases considered with two-step chemistry. The major species profiles (not plotted) agree so closely as to be almost indistinguishable, save for the small perturbations associated with the DNS data. The only significant differences exist in the comparison of predictions and observations for the radical species (H) and temperature.

A comparison of conditional mean H mass fraction profiles for various calculation times is plotted on the left-hand side of Fig. 7. It is clear that the CMC model overpredicts the level of H present, but the relative degree of overprediction at the peak mass fraction decreases with time as the magnitude of the profiles decreases. It also seems that the overprediction of conditional mean scalar dissipation rate at

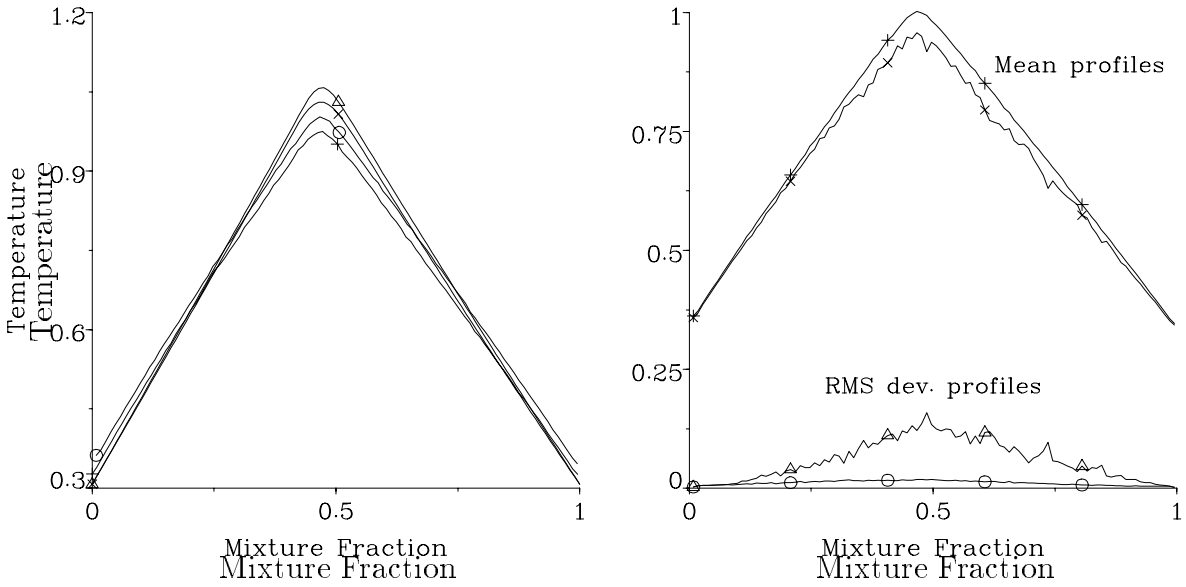

FIGURE 8. Comparison of modeled and observed conditional statistics for temperature at different calculation times. (Left) Modeled and observed mean profiles from two-step chemistry cases : + - DNS at $t/\tau_t = 1/3$, ∘ - DNS at $t/\tau_t = 1$, × - CMC at $t/\tau_t = 1/3$, △ - CMC at $t/\tau_t = 1$. (Right) Observed mean and RMS deviations at $t/\tau_t = 1$ in one- and two-step chemistry cases : + - mean from two-step, × - mean from one-step, ∘ RMS dev. from two-step, △ - RMS dev. from one-step.

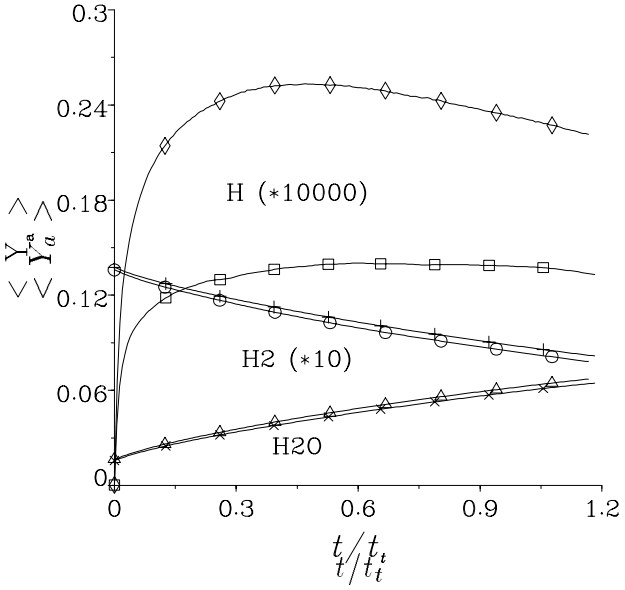

FIGURE 9. Time history of unconditional mean chemical yields from model and simulation : ⊓ - DNS $H(*10000)$, ♢ - CMC $H(*10000)$, ∘ - DNS $H_2(*10)$, + - CMC $H_2(*10)$, × - DNS H_2O, △ - CMC H_2O.

very rich mixture fractions, noted earlier, tends to cause the predicted H profile to be flattened at rich mixture fractions. In the right-hand plot of Fig. 7, the observed root mean square deviation profiles are plotted in comparison with the mean profiles. From this plot it appears that the absolute level of the deviational profiles decreases with time in accordance with the mean profiles.

On the left-hand side of Fig. 8, conditional mean temperature profiles are compared for various times in the CMC and DNS two-step chemical calculations. The model profiles are somewhat higher than the DNS measured profiles; however, the difference is substantially less than that seen in the one-step chemistry case. Also in contrast to the one-step chemistry comparison, both sets of profiles increase in magnitude with time. This is another indication of the fact that the two-step formulation gives rise to a chemical system that is less perturbed by mixing processes when compared to a similar case with one-step chemistry. This fact is highlighted in the right-hand plot of Fig. 8, where conditional mean temperature data is compared between DNS simulations with one- and two-step chemistry at a time of $t = \tau_t$. Not only is the mean profile greater in the two-step case, but the corresponding root mean square deviation profile is much lower.

It appears that the more robust nature of the two-step chemical mechanism lends itself better to CMC modeling, in the cases studied here, than its one-step counterpart. This is because the two-step mechanism is less perturbed by the level of mixing intensity with consequently smaller mixing induced deviations from the conditionally averaged reactive scalar values. This reduction in the size of conditional deviations thus improves the accuracy of the conditional mean chemical closure.

It is reasonable to assert that under more intense mixing conditions, that CMC models employing the two-step chemical mechanism would deviate to a larger degree from corresponding DNS observations. At very much higher mixing rates, the first order chemical closure would be invalidated altogether as the chemical system verges on extinction (see Bilger 1991, 1993).

3.2 Observed differential diffusion behavior

All of the DNS data and model predictions presented so far have been restricted to cases with uniform molecular diffusivity for all species ($Le_\alpha = 1$, $Pr = 0.75$). The DNS data presented in this section was computed with constant non-uniform Lewis numbers determined from counterflow laminar diffusion flames (see Smooke 1990). A Fickian diffusion approximation was used for all species, except nitrogen, which was the predominant background species for which the Lewis numbers were defined.

One of the most notable aspects of comparing general simulation behavior, with and without differential diffusion, is the absence of a unique mixture fraction definition in the former case. Fig. 10 illustrates this fact by plotting the scatter of points for two different conserved scalars, one based upon the mass fraction of an inert species (N_2) and the other based upon a combination of hydrogen and oxygen atomic mass fractions, at a time of $t/\tau_t = 1$. Instead of adhering to the constant mixing line (unit-slope line passing through the origin), the computed points follow the characteristic sigmoidal (reversed in this case) trace of differentially diffused

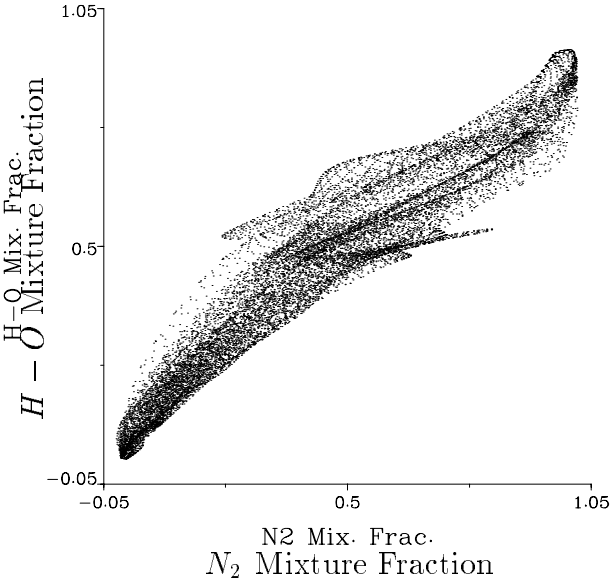

FIGURE 10. Scatter plot of mixture fractions based on N_2 mass fraction and H-O atomic mass fractions, for differential diffusion simulation at time $t/\tau_t = 1$.

conserved scalars. The reason for this behavior can be understood when it is revealed that the $H - O$ mixture fraction has a positive linear relation to the light hydrogen bearing species and a negative linear relation to the heavier oxygen bearing species. Being lighter and more mobile than the other species, H and H_2 tend to diffuse more rapidly to lean (N_2-based) mixture fractions than O_2 can diffuse to rich (N_2-based) mixture fractions. The result is that the $H - O$ mixture fraction values increases at lean N_2-based mixture fractions and simultaneously decrease at rich values.

The chemical yields of the two step chemistry simulations are compared for cases with and without differential diffusion in Fig. 11. It is apparent that the differential diffusion case predicts a slightly greater reactant consumption rate, but with a less discernible increase in major production formation. It would appear that the additional reactants consumed by the differential diffusion case go towards creating the obvious excess of the radical species H. The temperature and pressure traces for the two simulations are very close; however, the differential diffusion case appears to have very slightly lower values. A clear difference is apparent between the two unmixedness traces (unmixedness of normalized N_2 mass fraction), with the decay coefficient in the differential diffusion case being around ~ 0.86 of the coefficient in the uniform diffusivity case.

Conditional statistics were calculated using an N_2-based mixture fraction definition, and are plotted in Figs. 12 and 13 for H radical mass fraction and temperature, respectively. It is apparent from Fig. 12 that the conditional mean H radical profiles from the differentially diffusive (diff-diff) case are somewhat lower than the uniform diffusivity results on the rich side of stoichiometric. At the same time, the opposite

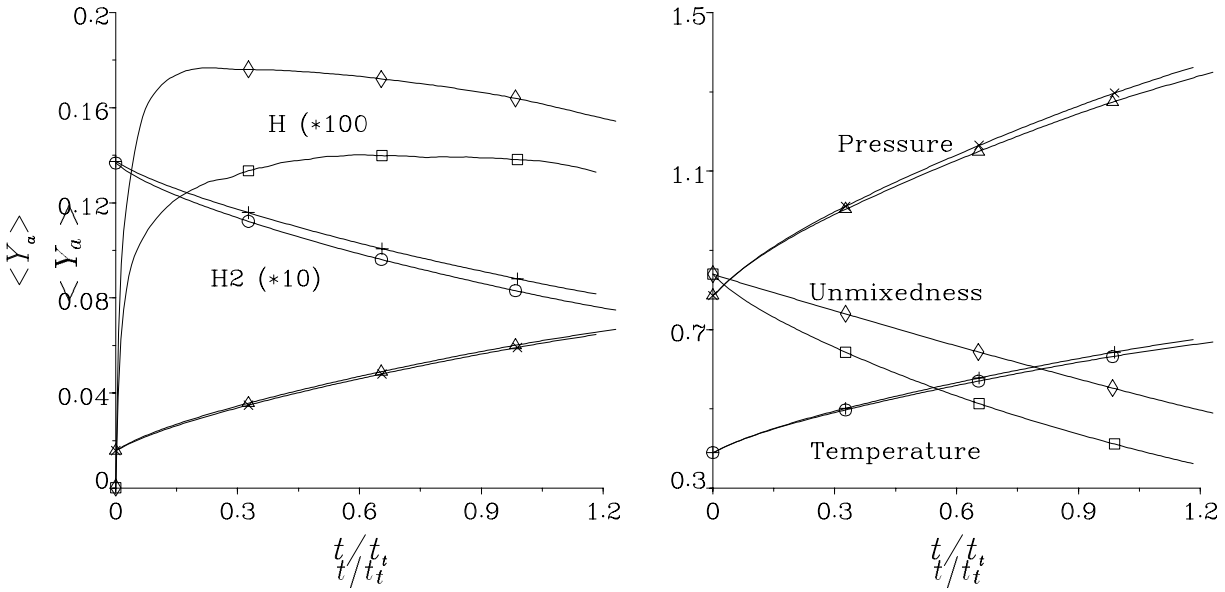

FIGURE 11. Time history of unconditional mean chemical yields from two-step chemistry simulations with and without differential diffusion. (Left) $\diamondsuit$ - dd $H(*10^5)$, $\sqcap$ - ud $H(*10^5)$, $\circ$ - dd $H_2(*10)$, $+$ - ud $H_2(*10)$, $\triangle$ - dd H_2O, $\times$ - ud H_2O. (Right) $\diamondsuit$ - dd unmixedness, $\sqcap$ - ud unmixedness, $\circ$ - dd temperature, $+$ - ud temperature, $\triangle$ - dd pressure, $\times$ - ud pressure.

is true on the lean side, where the differentially diffusive radicals have permeated this oxidizer-rich zone to a greater extent.

The mean temperature profiles from the diff-diff cases reflect the greater incursion of H radical into the lean zone, in that they are significantly elevated over the uniform diffusivity profiles. The presence of greater radical numbers allows the exothermic global reaction to proceed at a more rapid rate, thereby liberating more heat. It is clear that the root mean square deviations in the diff-diff case are much greater than in the corresponding uniform diffusivity cases. Since temperature is strongly dependent on reaction activity and this is in turn dependent on radical availability, these temperature deviations may be related to the disparate mixing behavior of H radical and N_2 (the conserved scalar) with the latter doing a poor job of tracking the mean transport of the former.

Finally it is interesting to compare the N_2-based mixture fraction PDFs observed in each simulation case. The PDFs plotted in Fig. 14 are from the time $t = \tau_t$ and embody the main difference between the diff-diff and uniform diffusivity behavior. The diff-diff PDF equation has a non-zero source term arising out the definition of N_2 mass fraction as the residual mass not accounted for by the reactive species mass fractions. This source term averages across mixture fraction space to provide a zero mean contribution, but serves to inflate the PDF at some mixture fractions. The source term (not plotted) has a sharp peak just to the lean side of stoichiometric, which results from H and H_2 incursion, and this peak causes the diff-diff case's

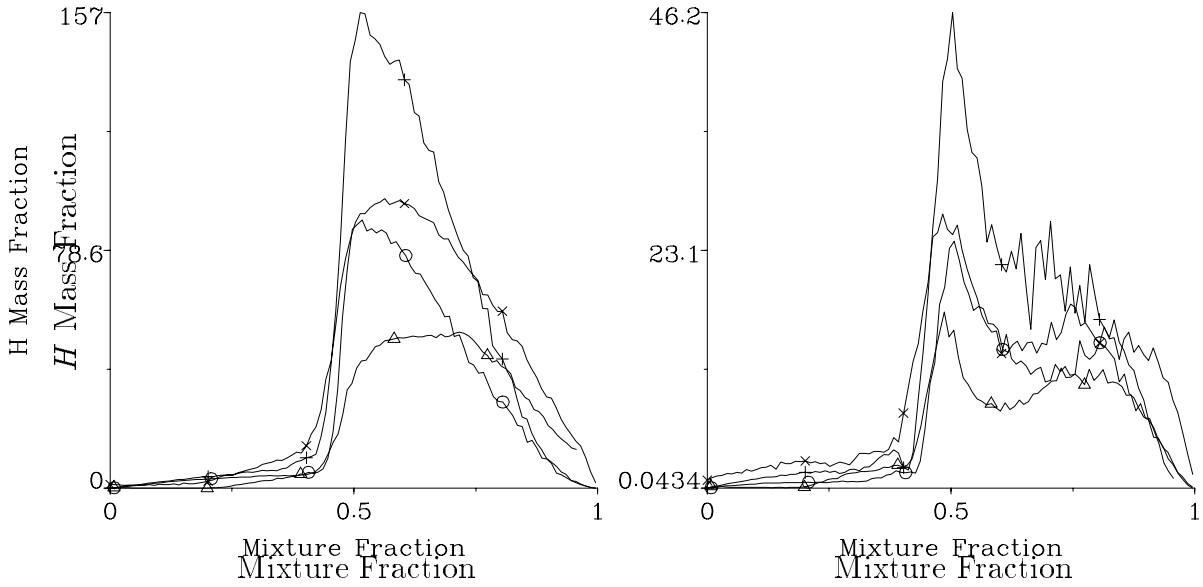

FIGURE 12. Comparison of observed conditional mean (left) and RMS deviations (right) for H radical mass fraction in cases with and without differential diffusion at different calculation times : + - ud at $t/\tau_t = 1/3$, $\times$ - dd at $t/\tau_t = 1/3$, $\circ$ - ud at $t/\tau_t = 1$, $\triangle$ - dd at $t/\tau_t = 1$.

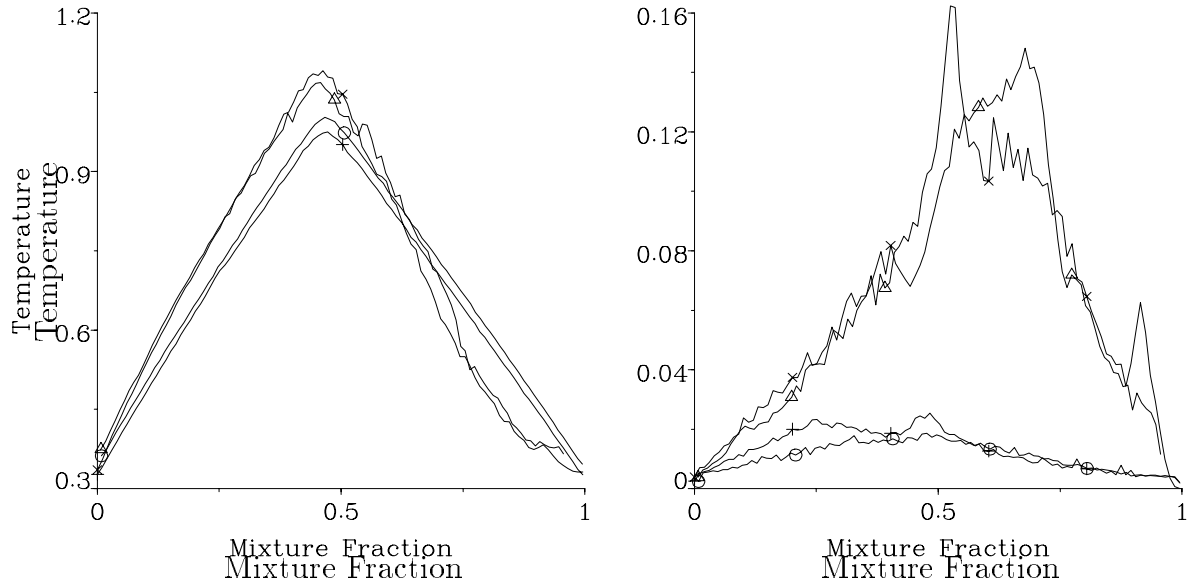

FIGURE 13. Comparison of observed conditional mean (left) and RMS deviations (right) for temperature in cases with and without differential diffusion at different calculation times : + - ud at $t/\tau_t = 1/3$, $\times$ - dd at $t/\tau_t = 1/3$, $\circ$ - ud at $t/\tau_t = 1$, $\triangle$ - dd at $t/\tau_t = 1$.

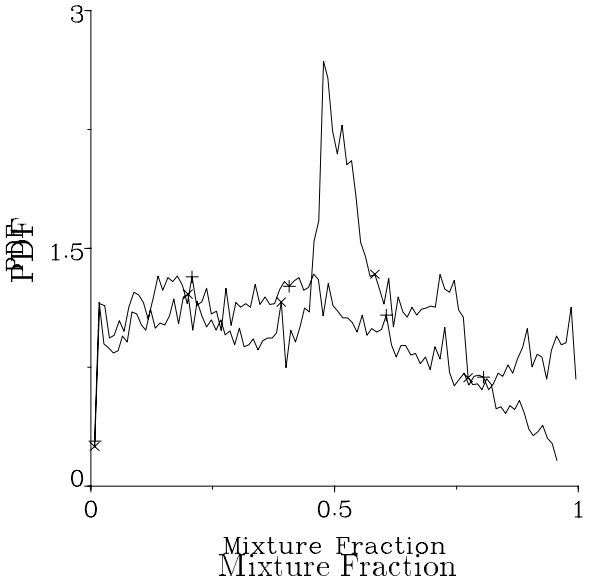

FIGURE 14. Comparison of N_2-based mixture fraction PDFs from uniform and non-uniform molecular diffusivity simulations at time $t = \tau_t$: + - uniform diffusivity, $\times$ - differential diffusivity

PDF to increase at this mixture fraction.

4. Discussion

Much of current turbulent nonpremixed combustion modeling relies on the existence of a unique mixture fraction, particularly the Joint PDF method (Pope 1985, 1991, Chen *et al.* 1990), and, of course, the CMC method (Smith 1994, Smith *et al.* 1995). Rationales have been put forth that suggest differential diffusion effects are small at high Reynolds numbers; however, experimental evidence suggests that they are substantial even in jet diffusion flames with Reynolds numbers as high as 30000 (Smith *et al.* 1993).

Let us briefly examine the impact of differential diffusion on the CMC method and discuss the additional modeling issues which arise. The equation for a composite conserved scalar ($\xi \equiv \sum_{\alpha=1}^{N} a_\alpha Y_\alpha$) is given by,

$$\frac{\partial}{\partial t}(\rho\xi) + \frac{\partial}{\partial x_i}(\rho u_i \xi) = \frac{\partial}{\partial x_j}(\rho D_\xi \frac{\partial \xi}{\partial x_j}) + \dot{s}_\xi \tag{15}$$

where $\dot{s}_\xi$ is a differential diffusion source term equal to

$$\dot{s}_\xi \equiv \frac{\partial}{\partial x_j}(\rho \sum_{\alpha=1}^{N} a_\alpha (D_\alpha - D_\xi) \frac{\partial Y_\alpha}{\partial x_j}). \tag{16}$$

From this equation it can be shown that the corresponding PDF equation is given by,

$$\frac{\partial}{\partial t}(< \rho \mid \eta > P_\eta) + \frac{\partial}{\partial x_i}(< \rho u_i \mid \eta > P_\eta) + e_\xi \tag{17}$$

and following the methodology of Klimenko (1990) yields the following CMC equation.

$$< \rho \mid \eta > \frac{\partial Q_\alpha}{\partial t} + < \rho u_i \mid \eta > \frac{\partial Q_\alpha}{\partial x_i} = \frac{1}{2} < \rho\chi \mid \eta > \frac{\partial^2 Q_\alpha}{\partial \eta^2} + < \rho \dot{w}_{\ alpha} \mid \eta > + e_q^* + e_Q^* \tag{18}$$

The residual terms e_q^* and e_Q^* are defined as,

$$e_q^* \equiv \frac{1}{P_\eta}[\frac{\partial}{\partial x_j}(< \rho u_i' y_\alpha' \mid \eta > P_\eta) - \frac{\partial}{\partial \eta}(< \dot{s}_\xi' y_\alpha' \mid \eta > P_\eta)] \tag{19}$$

and

$$e_Q^* \equiv < \frac{\partial}{\partial x_j}(\rho(D_\alpha - D_\xi)\frac{\partial Y_\alpha}{\partial x_j} \mid \eta > - < \dot{s}_\xi \mid \eta > \frac{\partial Q_\alpha}{\partial \eta}. \tag{20}$$

The additional terms in the CMC and PDF equations are dependent on the definition of mixture fraction selected as the conditioning variable. Note that the e_Q^* term becomes small at high Reynolds numbers, but it is not clear that the same can be said for e_q^*.

The choice of a conserved scalar as a conditioning variable is governed by two criteria. Firstly, the scalar should be representative of the molecular transport of as many important chemical species as possible so as to minimize deviations from the resultant conditional averages. Secondly, in order to be able to model the evolution of the conserved scalar PDF (and thereby determine $< \rho\chi \mid \eta >$) in a simple manner, the mixture fraction source term $\dot{s}_\xi$ should be as small as possible. These criteria may prove to be conflicting. For example, it is possible to use an inert tracer species as a conserved scalar, thereby making $\dot{s}_\xi$ identically zero, but as this definition does not include any of the reactive species that are being tracked, deviations from the conditional means may be too great to effect a chemical source term closure.

Klimenko (1994) provides an equation for the conditional mean square deviation θ_α from a conditional mean reactive scalar Q_α in isotropic turbulence. This equation is slightly modified in the presence of differential molecular diffusivity to become,

$$< \rho \mid \eta > \frac{\partial \theta_\alpha}{\partial t} - \frac{1}{2} < \rho\chi \mid \eta > \frac{\partial \theta_\alpha}{\partial \eta} = < \rho \dot{w}_\alpha' y_\alpha' \mid \eta > -2 < D_\alpha (\frac{\partial y_\alpha'}{\partial x_i})^2 \mid \eta > + e_\theta^* + e_\Theta^*. \tag{21}$$

where the residual terms are analogous to e_q^* and e_Q^* but involve the conditional mean deviation rather than the conditional mean. The instantaneous change and transport of the conditional mean deviation is balanced against a chemical-instability source term, a deviational dissipation term, and residuals. Where the Reynolds number is moderate and the choice of conserved scalar is poor, the residuals will tend to increase the level of deviations. When combined with the nonlinear amplification provided by the chemical term, this added source of conditional deviation can cause levels to increase substantially (see Section 3.2) and thereby invalidate any first order chemical closure.

It may be that the chemical source term $< \rho \dot{w}_\alpha \mid \eta >$ can be closed using a second order method such as that applied by Li and Bilger (1993) to atmospheric pollutant

reactions in a turbulent mixing layer. However, in that case the chemistry was isothermal and one-step in nature and did not have significant differential diffusion. At higher Reynolds numbers the effect of differential diffusion is diminished, and it may be that practical devices that can be highly turbulent do not require a diff-diff treatment. At higher Reynolds numbers, however, deviations arise in Eq. 21 because of mixing interference via the chemical instability term (see Section 3.1), and it may be necessary to develop doubly conditional moment closures in order to model these conditions.

5. Conclusions and future plans

In this study, predictions from the CMC method for modeling turbulent nonpremixed combustion were compared to DNS data for hydrogen burning in an isotropic decaying turbulent field. One- and two-step chemical mechanisms were used in both the model and simulation in order to study the effect of chemical complexity upon first order CMC chemical closure.

It was found that the one-step chemical mechanism was hindered to a greater extent over the two-step mechanism, under identical mixing conditions, as a result of a breakdown in the one-step assumption for radical partial equilibrium. This interference by the mixing processes lead to larger deviations from conditional mean reactive scalar profiles. This in turn made the one-step chemical system harder to model with the CMC method than the two-step system under the same mixing conditions.

The addition of differential molecular diffusivity to the analysis tended to increase the level of reactive scalar deviations from conditional means under the conditions studied. The different rates of species transport tended to modify the overall rate of chemical reaction in the hydrogen system. The lack of a unique conserved scalar as a conditioning variable caused conditional mean scalar profiles to shift in mixture fraction space according to the choice of conserved scalar.

It was suggested that the increase in conditional deviations that arise from differential diffusion effects is a potential source of serious in implementing a conditionally averaged first order chemical closure.

The future plan for this modeling project can be outlined as follows:

- Perform three-dimensional simulation under same kind of conditions to include the vortex stretching mechanism and improve the size of the statistical sample.
- Develop model refinements for treating differential diffusion—may require solving for conditional deviations.
- Investigate doubly-conditional moment closure methods in spatially degenerate case. This will allow high intensity near-extinction behavior to be examined.
- Use flexible chemical module for other mechanisms such as $H_2 - CO$.

REFERENCES

Bilger, R. W. 1982 Molecular Transport Effects in Turbulent Diffusion Flames at Moderate Reynolds Number. *J AIAA*, **20**, 962-970.

BILGER, R. W. 1989 Turbulent Diffusion Flames. *Ann. Rev. Fluid. Mech.*, **21**, 101-135.

BILGER, R. W. 1991 Conditional Moment Methods for Turbulent Reacting Flow using Crocco Variable Conditions. *Charles Kolling Report TNF99*, the University of Sydney.

BILGER, R. W. 1993 Conditional Moment Methods for Turbulent Reacting Flow. *Phys. Fluids*, **5**, 436-444.

CHEN, J.-Y., DIBBLE, R. W., BILGER, R. W. 1990 PDF Modelling of Turbulent Nonpremixed CO/H2/N2 Jet Flames with Reduced Mechanisms. *Twenty-Third Symposium (International) on Combustion*, the Combustion Institute, Pittsburgh, 775-780.

CORREA, S. M. 1993 A Review of NOx Formation under Gas-Turbine Combustion Conditions. *Comb. Sci. Tech.*, **87**, 329-362.

GIRIMAJI, S. S. 1991 Assumed Beta-pdf Model for Turbulent Mixing: Validation and Extension to Multiple Scalar Mixing. *Comb. Sci. and Tech.*, **78**, 177-196.

KLIMENKO, A. YU. 1990 Multicomponent Diffusion of Various Admixtures in Turbulent Flow. *Fluid Dynamics* **25**, 327-334.

KLIMENKO, A. YU. 1992 Conditional Moment Closure and Diffusion in Conserved Scalar Phase Space. *ECOLEN Scientific Research Lab Paper*, Moscow, Russia.

KLIMENKO, A. YU. 1994 Conditional Moment Closure and Large-Scale Fluctuations of Scalar Dissipation. *Fluid Dynamics*, **28**, 630-637.

KLIMENKO, A. YU., BILGER, R. W. 1992 Relationship between conserved scalar pdfs and scalar dissipation in turbulent flows. *Charles Kolling Report TNF101*, the University of Sydney.

LELE, S. 1992 Compact finite difference schemes with spectral-like resolution. *J. Comp. Phys.* **103**, 16.

LI, J. D., BILGER, R. W. 1993 Measurement and Predictions of the Conditional Variance in a Turbulent Reactive-Scalar Mixing Layer. *Phys. of Fluids*, **5**, 3255-3264.

MANTEL, T., 1994 Fundamental mechanisms in premixed flame propagation via vortex-flame interactions - numerical simulations. *Annual Research Briefs - 1994*, Center for Turbulence Research, NASA Ames/Stanford Univ.

POINSOT, T., LELE, S. 1992 Boundary conditions for direct simulations of compressible viscous flows. *J. Comp. Phys.*, **101**, 104.

POPE, S. B. 1985 PDF Methods for Turbulent Flows. *Prog. Energy Comb. Sci.*, **11**, 119-192.

POPE, S. B. 1991 Computations of Turbulent Combustion: Progress and Challenges. *Twenty-Third Symposium (International) on Combustion*, Combustion Institute, Pittsburgh. 591-612.

RUETSCH, G. R. 1994 Flame propagation under partially premixed conditions. *Annual Research Briefs - 1994*, Center for Turbulence Research, NASA Ames/Stanford Univ.

SMITH, L. L., DIBBLE, R. W., TALBOT, L., BARLOW, R. S., CARTER, C. D. 1993 Laser Raman Scattering Measurements of Differential Molecular Diffusion in Turbulent Nonpremixed Jet Flames of H_2/CO_2 Fuel. *Comb. Flame*, **100**, 153-160.

SMITH, N. S. A. 1994 *Development of the Conditional Moment Closure Method for Modelling Turbulent Combustion.* PhD Thesis, University of Sydney.

SMITH, N. S. A., BILGER, R. W., CARTER, C. D., BARLOW, R. S., CHEN, J.-Y., 1995 A Comparison of CMC and PDF Modelling Predictions with Experimental Nitric Oxide LIF/Raman Measurements in a Turbulent H_2 Jet Flame. *Comb. Sci. Tech.*, **105**, 357-375.

VERVISCH, L. 1992 Study and modeling of finite rate chemistry effects in turbulent nonpremixed flames. *Annual Research Briefs - 1992*, Center for Turbulence Research, NASA Ames/Stanford Univ.

YEUNG, P. K., POPE, S. B. 1993 Differential Diffusion of Passive Scalars in Isotropic Turbulence. *Phys. Fluids*, **5**, 2467-2478.